

Analysis of the $q\bar{q} \rightarrow Z^* \rightarrow hA \rightarrow 4\tau$ process within the lepton-specific 2HDM at the LHC

Yan Ma,^{1,*} A. Arhrib,^{2,†} S. Moretti,^{3,‡} S. Semlali,^{4,§} Y. Wang,^{5,¶} and Q.S. Yan^{6,**}

¹*College of Physics and Electronic Information,*

Inner Mongolia Normal University, Hohhot 010022, PR China

²*Abdelmalek Essaadi University, Faculty of Sciences and Techniques, B.P. 2117 Tétouan, Tanger, Morocco &*

Department of Physics and Center for Theory and Computation,

National Tsing Hua University, Hsinchu, Taiwan 300

³*School of Physics & Astronomy, University of Southampton, Southampton SO17 1BJ, UK &*

Department of Physics & Astronomy, Uppsala University, Box 516, 75120 Uppsala, Sweden

⁴*School of Physics and Astronomy, University of Southampton, Southampton SO17 1BJ, UK &*

Particle Physics Department, Rutherford Appleton Laboratory,

Chilton, Didcot, Oxon OX11 0QX, United Kingdom

⁵*College of Physics and Electronic Information,*

Inner Mongolia Normal University, Hohhot, 010022, China &

Key Laboratory for Physics and Chemistry of Functional Materials,

Inner Mongolia Normal University, Hohhot, 010022, China

⁶*Center for Future High Energy Physics, Chinese Academy of Sciences, Beijing 100049, PR China &*

School of Physics Sciences, University of Chinese Academy of Sciences, Beijing 100039, PR China

Abstract

We analyse light Higgs scalar and pseudoscalar associated hadro-production in the 2-Higgs Doublet Model (2HDM) Type-X (or lepton-specific) within the parameter space allowed by theoretical self-consistency requirements as well as the latest experimental constraints from the Large Hadron Collider (LHC), precision data and B physics. Over the viable regions of such a scenario, the Standard Model-like Higgs boson discovered at the LHC in 2012 is the heavier CP-even state H . Furthermore, in the Type-X scenario, due to large $\tan\beta$, the lighter Higgs scalar h and the pseudoscalar A mainly decay into two τ leptons. Therefore, we concentrate on analysing the signal process $pp \rightarrow Z^* \rightarrow hA \rightarrow \tau^+\tau^-\tau^+\tau^- \rightarrow \ell\nu_\ell\ell\nu_\ell\tau_h\tau_h$ (where $\ell = e, \mu$ whereas τ_h represents the hadronic decay of the τ) and explore the feasibility of conducting such a search at the LHC with a centre-of-mass energy of $\sqrt{s} = 14$ TeV and a luminosity of $L = 300 \text{ fb}^{-1}$. To suppress the huge SM background, we confine ourselves to consider the fraction of signal events with two same-sign τ leptons further decaying into same-sign leptons while the other two τ leptons decay hadronically. We find that a combination of kinematical selection and machine learning (ML) analysis will yields significant sensitivity to this process at the end of the LHC Run 3.

KEYWORDS: 2-Higgs Doublet Model, Type-X Scenario, Higgs Physics

* 20214016005@mails.imnu.edu.cn

† a.arhrib@gmail.com

‡ s.moretti@soton.ac.uk; stefano.moretti@physics.uu.se

§ s.semlali@soton.ac.uk

¶ wangyan@imnu.edu.cn

** yanqishu@ucas.ac.cn

CONTENTS

I. Introduction	2
II. The 2HDM	4
III. Bounds and constraints in the parameter space scans	6
IV. Collider phenomenology	8
A. Event generation and selection	9
B. Event reconstruction	11
C. Multivariate analysis	15
D. Significances	17
V. Conclusions	19
Acknowledgments	19
References	19

I. INTRODUCTION

The LHC has played an indispensable role in improving our understanding of the micro-cosmic subatomic structure, particularly with the discovery of a 125 GeV scalar particle by the ATLAS and CMS experimental teams in 2012 [1, 2]. This was the last particle predicted by the Standard Model (SM) and its properties measured in the above experiments are currently consistent with the SM prediction at the 5σ level [3, 4]. Investigating the Higgs sector at the LHC, where the presence of additional (pseudo)scalars is possible, remains an intriguing task, particularly in new physics models with additional doublet fields. Therefore, to discover extra Higgs bosons at the LHC is one of the prime targets of Beyond the SM (BSM) signal searches.

One of the simplest extensions of the SM is the 2HDM, which contains two complex Higgs doublets [5–7]. After Electro-Weak Symmetry Breaking (EWSB), there are three Goldstone bosons, which are ‘eaten’ by the W^\pm and Z bosons while the remaining five degrees of freedom incarnate into physical Higgs bosons: two neutral CP-even scalars (h and H , with

$M_h < M_H$), one CP-odd pseudoscalar (A) and two charged Higgs states H^\pm (with mixed CP status).

In order to be consistent with the stringent experimental constraints from Flavour Changing Neutral Currents (FCNCs) at the tree level, typically, a Z_2 symmetry is introduced into the Yukawa sector so that each type of fermion only couples to one of the doublets of the 2HDM [8]. Based on the Z_2 charge assignments of the Higgs doublets, we can define four basic scenarios, known as (Yukawa) types. In the lepton-specific scenario (or Type-X), the additional Higgs doublet ϕ_2 only couples to the lepton sector and not to the quark sector, where the light Higgs boson mainly decays to $\tau^+\tau^-$ within a wide range of parameter spaces [9].

Motivated by recent searches for $\tau^+\tau^-\tau^+\tau^-$ by the CMS experiment [10–12], we will study the process $pp \rightarrow Z^* \rightarrow hA \rightarrow \tau^+\tau^-\tau^+\tau^-$ in the 2HDM Type-X. In this scenario, the $h/A \rightarrow \tau^+\tau^-$ decay could be enhanced, resulting in a sizeable 4τ final state. Therefore, it is worthwhile to examine whether this statement is robust enough after taking into account the effects of parton shower, hadronisation, heavy flavour decays and detector resolution.

The recent results by the (muon) $g - 2$ experiment conducted by the Fermilab National Accelerator Laboratory (FNAL), when combined with the old ones from the Brookhaven National Laboratory (BNL), yield a 4.2σ discrepancy between the experimental data and the theoretical prediction from the SM:

$$\Delta a_\mu = a_\mu^{\text{exp}} - a_\mu^{\text{SM}} = (25.1 \pm 5.9) \times 10^{10}, \quad (1)$$

where $a_\mu = (g - 2)_\mu/2$ [13]. One can explain this using 2HDM Type-X model, though, since the couplings of the new Higgs bosons to the SM fermions are proportional to $\tan\beta$, thereby enhancing the corresponding contributions to Δa_μ [14]. Although a recent measurement has already shown possibilities of restricting the parameter spaces of the Type-X model in the large $\tan\beta$ region [15], further research is still required to be performed.

In this paper, we assume that the heavier CP-even Higgs boson H is the observed SM-like Higgs boson whose properties agree with the LHC measurements. We then perform a detailed Monte Carlo (MC) study on the signal process $pp \rightarrow Z^* \rightarrow hA \rightarrow 4\tau \rightarrow l\nu_l l\nu_l \tau_h \tau_h$ (with $l = e, \mu$ and τ_h representing hadronic τ -decays) and relevant background processes, to examine its feasibility at the LHC. We do so after taking into account relevant theoretical and experimental conditions. In order to improve the experimental significance,

we will require two Same-Sign (SS) leptons. Our analysis demonstrates that, by using this signature, the relevant parameter space can be either discovered or ruled out by using the current integrated luminosity at the LHC.

The paper is organised as follows. In the next section, we briefly describe the 2HDM and its Yukawa scenarios, then introduce a few Benchmark Points (BPs) for our MC analysis which pass all present theoretical and experimental constraints. In the following section, we perform a detailed collider analysis of these BPs and examine the potential to discover the aforementioned signature within the 2HDM Type-X scenario. Finally, we present some conclusions.

II. THE 2HDM

The Higgs sector of the 2HDM consists of two weak isospin doublets with hypercharge $Y = 1$. The most general Higgs potential for the 2HDM that complies with the $SU(2)_L \times U(1)_Y$ gauge structure of the EW sector of the SM has the following form [7]:

$$\begin{aligned}
V(\phi_1, \phi_2) = & m_{11}^2(\phi_1^\dagger\phi_1) + m_{22}^2(\phi_2^\dagger\phi_2) - [m_{12}^2(\phi_1^\dagger\phi_2) + \text{h.c.}] \\
& + \frac{1}{2}\lambda_1(\phi_1^\dagger\phi_1)^2 + \frac{1}{2}\lambda_2(\phi_2^\dagger\phi_2)^2 + \lambda_3(\phi_1^\dagger\phi_1)(\phi_2^\dagger\phi_2) + \lambda_4(\phi_1^\dagger\phi_2)(\phi_2^\dagger\phi_1) \\
& + \frac{1}{2} \left[\lambda_5(\phi_1^\dagger\phi_2)^2 + \text{h.c.} \right] + \left\{ \left[\lambda_6(\phi_1^\dagger\phi_1) + \lambda_7(\phi_2^\dagger\phi_2) \right] (\phi_1^\dagger\phi_2) + \text{h.c.} \right\}, \quad (2)
\end{aligned}$$

where ϕ_1 and ϕ_2 are the two Higgs doublet fields. By hermiticity of such a potential, $\lambda_{1,2,3,4}$ as well as $m_{11,22}^2$ are real parameters, while $\lambda_{5,6,7}$ and m_{12}^2 can be complex, in turn enabling possible Charge and Parity (CP) violation effects in the Higgs sector. Upon enforcing two minimisation conditions of the potential, m_{11}^2 and m_{22}^2 can be replaced by $v_{1,2}$, which are the Vacuum Expectation Values (VEV) of the Higgs doublets $\phi_{1,2}$, respectively. Moreover, the coupling $\lambda_{1,2,3,4,5}$ can be substituted by the four physical Higgs masses (i.e., M_h, M_H, M_A and M_{H^\pm}) and the parameter $\sin(\beta - \alpha)$, where α and β are, respectively, the mixing angles between the CP-even states and the angle related to the VEV values, i.e., $\tan \beta = v_1/v_2$. Thus, independent input parameters can be taken as M_h, M_H, M_A and M_{H^\pm} , λ_6, λ_7 , $\sin(\beta - \alpha)$, $\tan \beta$ and m_{12}^2 .

If both Higgs doublet fields of the general 2HDM couple to all fermions, the ensuing scenario can induce FCNCs in the Yukawa sector at tree level. As intimated, to remedy this, a Z_2 symmetry is imposed on the Lagrangian such that each fermion type interacts

with only one of the Higgs doublets [8]. As a consequence, there are four possible types of 2HDM, namely Type-I, Type-II, Type-X (or lepton-specific) and Type-Y (or flipped). However, such a symmetry is explicitly broken by the quartic couplings $\lambda_{6,7}$ and softly broken by the (squared) mass term m_{12}^2 . In what follows, we shall consider a CP-conserving (i.e., m_{12}^2 and λ_5 are real) 2HDM Type-X and assume $\lambda_6 = \lambda_7 = 0$ to forbid explicit breaking of Z_2 while also taking m_{12}^2 to be generally small, thereby preventing large FCNCs at tree level, which are incompatible with experiment.

In general, the couplings of the neutral and charged Higgs bosons to fermions can be described by the Yukawa Lagrangian given by [7]

$$-\mathcal{L}_{\text{Yukawa}} = \sum_{f=u,d,l} \left(\frac{m_f}{v} \kappa_f^h \bar{f} f h + \frac{m_f}{v} \kappa_f^H \bar{f} f H - i \frac{m_f}{v} \kappa_f^A \bar{f} \gamma_5 f A \right) + \left(\frac{V_{ud}}{\sqrt{2}v} \bar{u} (m_u \kappa_u^A P_L + m_d \kappa_d^A P_R) d H^+ + \frac{m_l \kappa_l^A}{\sqrt{2}v} \bar{\nu}_L l_R H^+ + \text{h.c.} \right), \quad (3)$$

where κ_f^S ($S = h, H$ and A) are the Yukawa couplings of the fermion f in the 2HDM, which are illustrated in Tab. I for the Type-X under consideration. Here, V_{ud} refers to a Cabibbo-Kobayashi-Maskawa (CKM) matrix element and $P_{L,R}$ denote the left- and right-handed projection operators, respectively. The coupling of the two CP-even states h and H to the gauge bosons VV ($V = W^\pm, Z$) are proportional to $\sin(\beta - \alpha)$ and $\cos(\beta - \alpha)$, respectively. If we assume that either h or H can be the observed SM-like Higgs boson, the coupling to gauge bosons is obtained for h when $\cos(\beta - \alpha) \rightarrow 0$ and for H when $\sin(\beta - \alpha) \rightarrow 0$. Therefore, each scenario can explain the 125 GeV Higgs signal at the LHC. Following our works [16–19], we shall focus in the present paper on the scenario where H mimics the observed signal with mass ~ 125 GeV (as previously intimated).

	κ_u^S	κ_d^S	κ_ℓ^S
h	$\cos \alpha / \sin \beta$	$\cos \alpha / \sin \beta$	$-\sin \alpha / \cos \beta$
H	$\sin \alpha / \sin \beta$	$\sin \alpha / \sin \beta$	$\cos \alpha / \cos \beta$
A	$\cot \beta$	$-\cot \beta$	$\tan \beta$

TABLE I. Yukawa couplings of the fermions $f = u, d$ and ℓ to the neutral Higgs bosons $S = h, H$ and A in the 2HDM Type-X.

III. BOUNDS AND CONSTRAINTS IN THE PARAMETER SPACE SCANS

To determine the regions that meet both theoretical requirements and experimental observations, the subsequent numerical explorations of the potential parameter spaces have been carried out:

$$\begin{aligned}
 M_h &\in [90, 125] \text{ (GeV)}, & M_H &= 125 \text{ (GeV)}, & M_A &\in [90, 125] \text{ (GeV)} \\
 M_{H^\pm} &\in [90, 125] \text{ (GeV)}, & \sin(\beta - \alpha) &\in [-0.25, 0.05], & \tan\beta &\in [20, 200] \\
 m_{12}^2 &= M_{H^\pm}^2 \frac{\tan\beta}{1 + \tan^2\beta} \text{ (GeV)}^2.
 \end{aligned} \tag{4}$$

The program `2HDMC-1.8.0` [20] was employed to calculate the Higgs branching ratios (BRs) and to examine the following theoretical and experimental constraints.

- Vacuum stability [6]: the scalar potential should be bounded by the conditions $\lambda_1 > 0$, $\lambda_2 > 0$, $\lambda_3 > -\sqrt{\lambda_1\lambda_2}$ and $\lambda_3 + \lambda_4 - \lambda_5 > -\sqrt{\lambda_1\lambda_2}$.
- Perturbativity constraints [24, 25], which imply the condition $|\lambda_i| < 8\pi$, which holds for $i = 1$ to 5.
- Tree-level perturbative unitarity [23–25]: requiring all $2 \rightarrow 2$ scattering processes involving Higgs and gauge bosons at high energy to be unitary.
- Oblique EW parameters (S , T and U) [26, 27], which govern the mass splitting between the Higgs states, with the following measured values [28]:

$$S = -0.02 \pm 0.10, \quad T = 0.03 \pm 0.12. \tag{5}$$

The correlation factor between S and T is set to 0.92 for consistency at 95% Confidence Level (CL).

To account for potential additional Higgs bosons, exclusion bounds at 95% CL are enforced using the `HiggsBounds-5.9.0` program [29], which systematically checks each parameter point against the 95% CL exclusion limits derived from Higgs boson searches conducted by LEP, Tevatron and LHC experiments.

To ensure agreement with the measurements of the SM-like Higgs state, constraints are enforced using the `HiggsSignals-2.6.0` program [30], which incorporates the combined measurements of the SM-like Higgs boson from LHC Run-1 and Run-2 data.

The constraints of flavour physics are incorporated using **SuperIso v4.1** [31] using the following observables:

- $\text{BR}(B \rightarrow X_s \gamma) = (3.32 \pm 0.15) \times 10^{-4}$ [35],
- $\text{BR}(B^0 \rightarrow \mu^+ \mu^-)_{(\text{LHCb})} = (1.2^{+0.8}_{-0.7}) \times 10^{-10}$ [36, 37],
- $\text{BR}(B^0 \rightarrow \mu^+ \mu^-)_{(\text{CMS})} = (0.37^{+0.75}_{-0.67}) \times 10^{-10}$ [38],
- $\text{BR}(B_s \rightarrow \mu^+ \mu^-)_{(\text{LHCb})} = (3.09^{+0.46}_{-0.43}) \times 10^{-9}$ [36, 37],
- $\text{BR}(B_s \rightarrow \mu^+ \mu^-)_{(\text{CMS})} = (3.83^{+0.38}_{-0.36}) \times 10^{-9}$ [38],
- $\text{BR}(B \rightarrow \tau \nu) = (1.09 \pm 0.20) \times 10^{-4}$ [35].

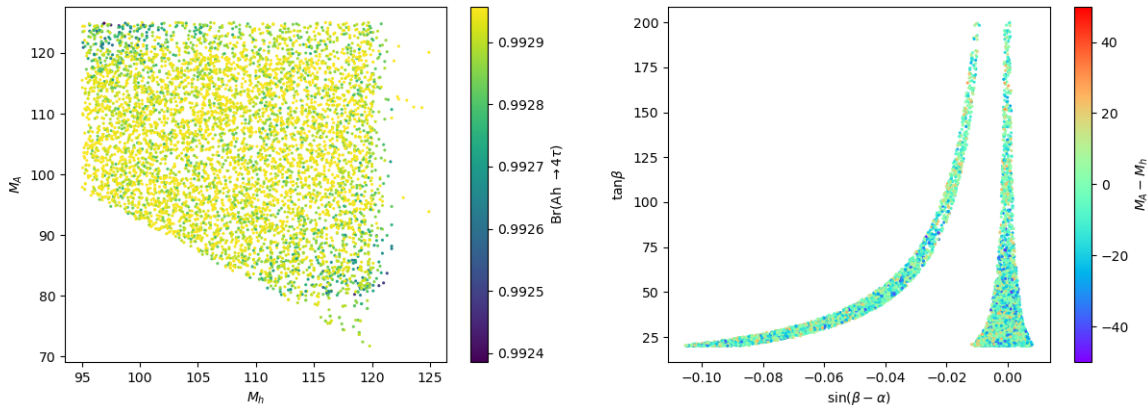


FIG. 1. Scatter plot of $\text{BR}(h \rightarrow \tau^+ \tau^-) \times \text{BR}(A \rightarrow \tau^+ \tau^-)$ as a function of M_h and M_A (left panel) and $M_A - M_h$ as a function of $\sin(\beta - \alpha)$ and $\tan\beta$ (right panel).

In the left panel of Fig. 1, we show the overall BR of the light Higgs h and the pseudoscalar A decaying into pairs of τ leptons, i.e., $\text{BR}(Ah \rightarrow 4\tau)$, within the allowed (M_h, M_A) plane of the 2HDM Type-X. Such a significant BR is attributable to the enhancement of the h/A couplings to leptons at large $\tan\beta$. The parameter spaces for $\sin(\beta - \alpha)$ and $\tan\beta$ are shown in the right panel, where the colour bar is $M_A - M_h$. It can be seen that most of the points are within the $M_A < M_h$ region.

When the constraint on a_μ is considered, there are two types of contributions to Δa_μ , which are one-loop corrections from H , A and H^\pm [32], as well as two-loop Barr-Zee contributions with heavy fermions [34]. Only in the large $\tan\beta$ regions Δa_μ is large enough to

explain the newest FNAL measurements. The surviving parameter space is shown in Fig. 2. Compared with Fig. 1 (left), most parameter spaces have been excluded; in fact, only points with $\tan\beta > 130$ are available, and the accessible (M_h, M_A) regions are rather sparse.

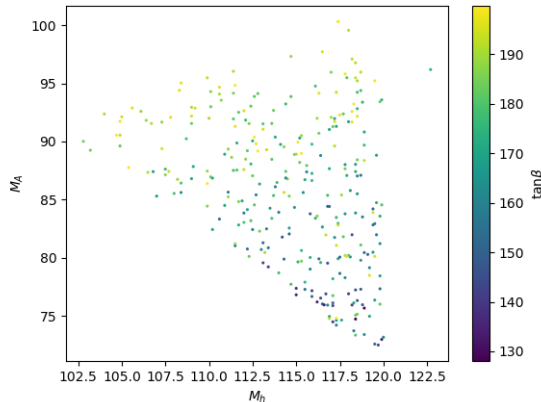


FIG. 2. Scatter plot of $\tan\beta$ as a function of M_h and M_A when the a_μ effect is considered in addition to the constraints imposed in the previous figure.

To test the allowed parts of the parameter space, nine BPs are given in the Tab. II, in terms of the 2HDM Type-X parameters entering our production and decay process, including the corresponding $pp \rightarrow Z^* \rightarrow hA \rightarrow 4\tau$ cross sections at the LHC with $\sqrt{s} = 14$ TeV. Based on this table, we select two scenarios. For BP1-4, where $\tan\beta$ always below 100 and $\sin(\beta - \alpha)$ is close to but not exactly zero. Here, a_μ remains a concern (till new measurements are performed) For BP5-9, the model is in the alignment-limit scenario, where $\sin(\beta - \alpha) = 0$ and $\tan\beta$ is very large. In this scenario, a_μ can be explained well (with the present measurements).

IV. COLLIDER PHENOMENOLOGY

In this section, we present a detailed MC analysis for both signal and background events at the detector level. In the $pp \rightarrow Z^* \rightarrow hA \rightarrow \tau^+\tau^-\tau^+\tau^- \rightarrow \nu_l\nu_l\nu_l\tau_h\tau_h$ process, i.e., the light Higgs (pseudo)scalar decays into two τ leptons and one of the τ 's decays into a charged lepton and neutrino, while the other τ decays hadronically (thus labeled as τ_h).

The main SM backgrounds are: $t\bar{t} \rightarrow \nu_l\nu_l b\bar{b}$, $W^\pm tb \rightarrow \nu_l\nu_l b\bar{b}$ (where the W^\pm boson and the b jet are not from a top quark resonance), $WWjj \rightarrow \nu_l\nu_l jj$, $Zjj \rightarrow \nu_l\nu_l jj$,

	M_h	M_A	M_{H^\pm}	$\tan \beta$	$\sin(\beta - \alpha)$	$\sigma_{4\tau, 14 \text{ TeV}} \text{ (fb)}$
BP1	95.10	121.70	95.02	24.19	-0.076	38.76
BP2	120.10	118.50	119.80	41.25	-0.003	27.89
BP3	99.52	102.30	99.53	60.71	-0.034	52.01
BP4	109.10	89.07	109.00	84.43	-0.025	55.23
BP5	105.70	117.40	105.60	105.30	-0.001	35.62
BP6	113.00	103.20	113.00	137.80	0.0	39.79
BP7	109.70	115.30	109.70	143.00	0.0	34.24
BP8	107.00	85.31	107.00	166.10	0.0	60.71
BP9	116.20	111.20	116.20	196.70	0.0	31.79

TABLE II. 2HDM Type-X input parameters and Leading Order (LO) cross sections (at the parton level with $\sqrt{s} = 14 \text{ TeV}$) are presented for each BP. The unit of all masses is GeV and we fix the SM-like Higgs boson mass as $M_H = 125 \text{ GeV}$. (Also recall that m_{12} has been taken as a derived quantity, function of M_{H^\pm} and $\tan \beta$.)

$ZZ \rightarrow \nu_l \nu_l \tau_h \tau_h$, $t\bar{t}Z \rightarrow \nu_l \nu_l b\bar{b}\tau\tau$, $t\bar{t}ZZ \rightarrow \nu_l \nu_l \nu_l \nu_l b\bar{b}\tau\tau$ and $t\bar{t}WW \rightarrow \nu_l \nu_l \nu_l \nu_l jj$. To suppress the huge SM background process Zjj , we deliberately choose two SS leptons plus two hadronic τ 's (for signal events, this is about 10% of the total number of 4τ ones). As a result, the final state consists of two SS leptons and two (light) jets.

A. Event generation and selection

We use MadGraph5_aMC@NLO v3.4.0 [39] to calculate cross sections and generate both signal and background events at the parton level. The following acceptance cuts are adopted for the signal and background generations:

$$|\eta(l, j)| < 2.5, \quad p_T(l, j) > 10 \text{ GeV}, \quad E_T^{\text{miss}} > 10 \text{ GeV}, \quad \Delta R(l, l, jj) > 0.4. \quad (6)$$

The parton-level events are then passed to Pythia [40, 41] to simulate initial- and final-state radiation (i.e. the QED and QCD emissions), parton shower, hadronisation and heavy flavour decays. We further use Delphes v3.4.2 [42] to simulate the detector effects. For each event, the anti- k_t jet algorithm [43] is used to cluster the jets with the jet parameter

$\Delta R = 0.4$ in the FastJet package [44]. The following kinematic cuts are further adopted in order to emulate the detector acceptance:

$$|\eta(l, j)| < 2.5, \quad p_T(l, j) > 10 \text{ GeV}. \quad (7)$$

The leptons are used for triggering purposes, so their kinematics must satisfy the trigger requirements¹.

Then, we select a final state consisting of two leptons and two jets from detector-simulated events. Tau tagging is not applied to improve the signal event rate. The signal results are presented in Tab. III and the relevant background processes are summarised in Tab. IV. The number of background events appears to be approximately 10^5 larger than the number of signal events, with the dominant background processes at this stage $pp \rightarrow t\bar{t}$ and $pp \rightarrow Zjj$.

To further suppress the huge SM backgrounds, we impose the selection condition requiring SS leptons. After applying this criterion, the number of signal and background events becomes comparable, with the dominant background contributions arising from the $pp \rightarrow t\bar{t}$ and $pp \rightarrow ZZ$ processes.

The cross sections of the signal and background processes after the detector acceptance cuts, the selection condition assuming a $2l2j$ final state, and plus the two SS leptons requirement are shown in Tabs. III and IV, respectively.

σ (fb)	BP1	BP2	BP3	BP4	BP5	BP6	BP7	BP8	BP9
Parton level	10.96	8.75	13.66	14.16	10.43	11.24	10.09	14.79	9.49
Selection of $2l2j$	3.02	2.59	3.66	3.68	2.87	3.20	2.95	3.83	2.67
Selection of SS $2l$	1.196	1.494	1.522	1.498	1.007	1.239	1.141	1.301	1.295

TABLE III. Cross sections for all signal BPs at the parton level as well as the detector level after selection cuts at the LHC with $\sqrt{s} = 14$ TeV.

¹ The CMS collaboration has developed a double-muon trigger to search for low P_T muons from B meson decays that are close together. A similar approach has been adopted recently to search for electron pairs from B meson decays, by tightening the topological selection criteria on the two Level-1 electron objects. In our recent paper [45], we explored the possibility of also developing an electron-muon trigger to search for low P_T leptons ($P_T \sim 10$ GeV).

σ (fb)	$t\bar{t}$	$W^\pm tb$	W^+W^-jj	Zjj	ZZ	$t\bar{t}Z$	$t\bar{t}ZZ$	$t\bar{t}W^+W^-$
Parton level	16060	518.3	1053	317600	18.89	0.49	1.14×10^{-4}	0.02
Selection of $2l2j$	8787.7	289.9	530.1	151086	10.0	0.33	1.1×10^{-4}	0.018
Selection of SS $2l$	19.43	0.62	1.99	0	2.51	0.079	3.3×10^{-5}	7.6×10^{-3}

TABLE IV. Cross sections for all backgrounds at the parton level as well as the detector level after selection cuts at the LHC with $\sqrt{s} = 14$ TeV.

In Fig. 3, the transverse momentum distributions of the (second-)leading jets (frame (a)) and leptons (frame (b)) are presented for the signal (e.g. BP4) and all background events. It is clear that the transverse momenta of the signal final state are always much softer than those for background events: This is because they emerge from rather light Higgs bosons, whose energies are capped at masses of the order of 100 GeV.

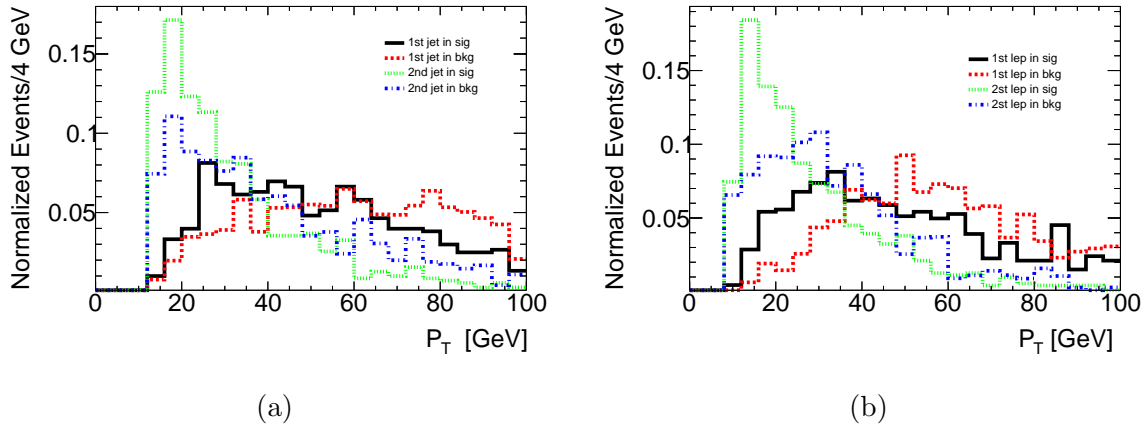


FIG. 3. Normalised distributions in transverse momentum of the first- and second-leading jets (a) and leptons (b) for BP4 and backgrounds at the LHC with $\sqrt{s} = 14$ TeV and $L = 300 \text{ fb}^{-1}$.

B. Event reconstruction

To further improve the signal-to-background discrimination, we reconstruct some kinematic features of signal events. However, it is extremely difficult to completely reconstruct the momentum of each light Higgs state. This is because each Higgs boson decays into two τ , with one of the τ 's decaying to a lepton and two neutrinos plus two τ neutrinos emerging from hadronic τ decays, leading to the presence of six neutrinos in a signal event.

Nevertheless, since the lepton momenta and the missing E_T (MET), where E_T refers to transverse energy, are all very small, we can approximately reconstruct the light Higgs bosons with only one lepton and one jet. Thus, there are two possible combinations with two leptons and two τ jets in each event. By defining a suitable χ^2 ,

$$\chi^2 = (M_{l_j^1}^1 - M_h)^2 + (M_{l_j^2}^2 - M_A)^2, \quad (8)$$

where $M_{h(A)}$ is the mass of the $h(A)$ (pseudo)scalar. We pair the two leptons and two jets to find a combination that minimises it and then assign these to $M_{l_j^1}^1$ and $M_{l_j^2}^2$, respectively. Since we did not consider neutrinos during such a mass reconstruction, the final $M_{l_j^1,2}^1,2$ values should be smaller than the real $M_{h/A}$ ones; see Figs. 4 frames (a) and (b). Taking again BP4 as an example, the reconstructed light Higgs mass distributions are shown in Fig. 4. A weak positive correlation was observed between these two variables (with r value of 0.27), as exemplified in Fig. 4 frame (c).

In order to further separate the signal from background events, we can also combine the two leptons and two jets, denoting their invariant masses as M_{ll} and M_{jj} , respectively. For some SM background processes, these lepton and/or jet pairs always come from some heavy resonance, i.e.. a top (anti)quark and a W^\pm or Z boson, the background spectra should have peaks in special mass regions. However, such a feature is largely removed when selecting SS leptons, as shown in Fig. 5, so it cannot really be exploited here.

We can further reconstruct the visible invariant mass, i.e. the one made up of the two leptons and two jets, M_{vis} , but without any MET. In the signal, these particles come from a virtual resonance Z^* , hence M_{vis} should be smaller than in the backgrounds, where this is not normally the case, the latter thus yielding a larger value; see Fig. 6 frame (a). Another useful kinematic variable is H_T , which is the scalar sum of the transverse momenta of the final-state objects, shown in Fig. 6 frame (b). These two observables are generated in a very similar way between signal and background, which is evident by comparing the two frames in this figure.

In our process, two neutrinos come from leptonic τ decays, hence very soft because the τ leptons are from cascade decays. There are also neutrinos in the backgrounds from W^\pm , Z boson or top (anti)quark (semi)leptonic decays, which have momenta higher than those of the neutrinos in signal events. The MET distribution is shown in Fig. 7 (a). Furthermore, the M_{T2} variable is often used to track the masses of unseen pairs of particles [46, 47], which

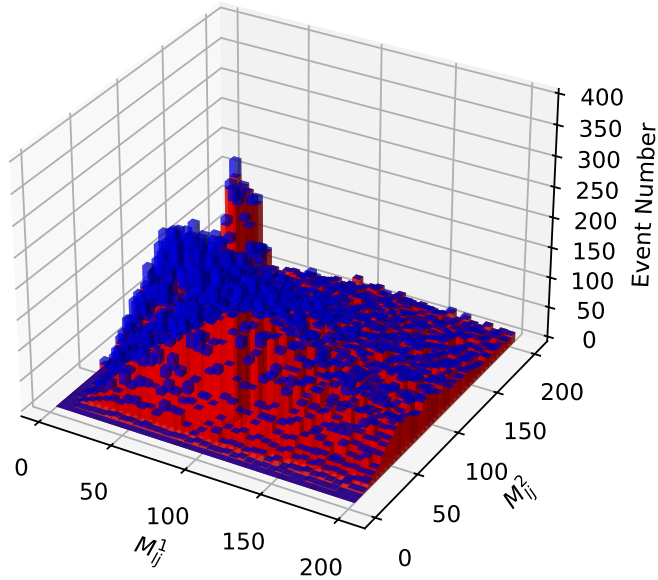
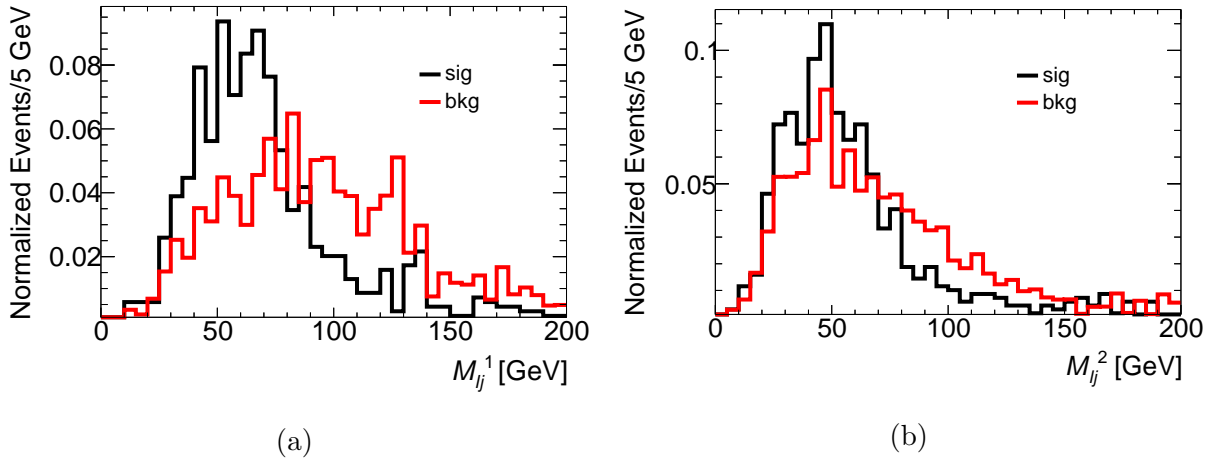


FIG. 4. Distributions in invariant mass of a lepton and a jet for BP4 and backgrounds at the LHC with $\sqrt{s} = 14$ TeV and $L = 300 \text{ fb}^{-1}$. The reconstructed values, corresponding to the best χ^2 fit, are labeled as M_{ij}^1 and M_{ij}^2 , which are normalised in (a) and (b), respectively, and unnormalised (for $L = 300 \text{ fb}^{-1}$) when correlated in (c). In the bottom frame the signal (background) is in blue(red).

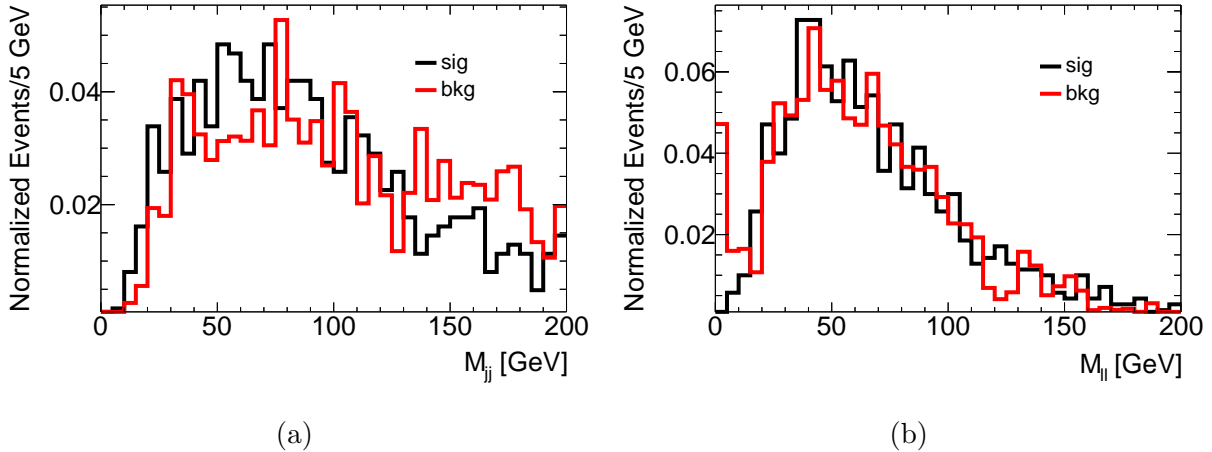


FIG. 5. Normalised distributions in invariant mass of lepton (a) and jet (b) pairs for BP4 and backgrounds at the LHC with $\sqrt{s} = 14$ TeV and $L = 300 \text{ fb}^{-1}$.

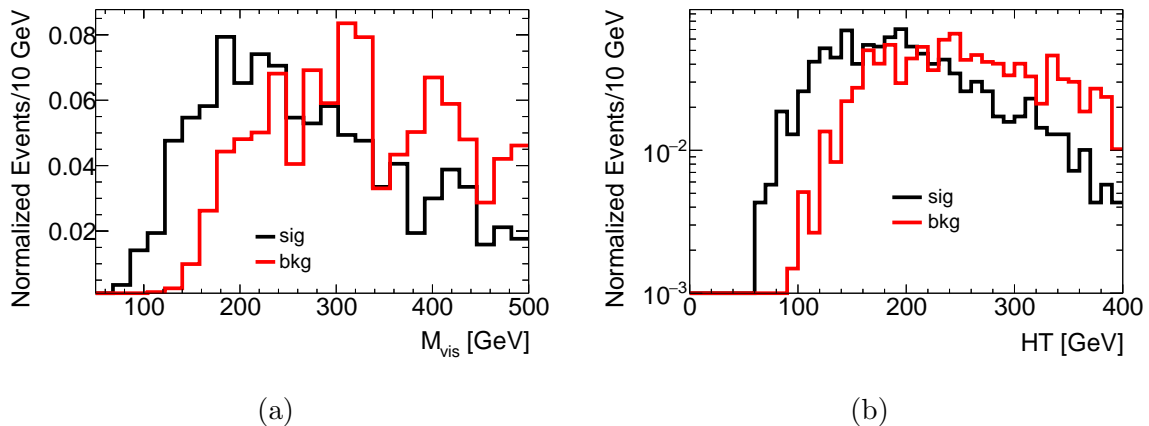


FIG. 6. Normalised distributions in visible invariant mass (a) and H_T (b) for BP4 and backgrounds at the LHC with $\sqrt{s} = 14$ TeV and $L = 300 \text{ fb}^{-1}$.

is defined as:

$$M_{T2}^2 \equiv \min_{p_1 + p_2 = p_T} [\max\{m_T^2(p_T^{lj^1}, p_1), m_T^2(p_T^{lj^2}, p_2)\}].$$

We thus reconstruct the M_{T2} variable for both signal and background, while splitting the latter into three classes: top (including $t\bar{t}$, $t\bar{t}W^+W^-$, $t\bar{t}Z$, $t\bar{t}ZZ$ events), W^\pm boson (including W^+W^-jj , $W^\pm tb$ events) and Z boson (including ZZ events). The M_{T2} distributions are shown in Fig. 7 (b). It can be seen that those of the signal and Z boson background are below 100 GeV or so while they are close to 150 GeV or so for the top quark and W^\pm boson processes. Thus, the M_{T2} variable provides an efficient discrimination, at least, against the top quark and W^\pm boson noises.

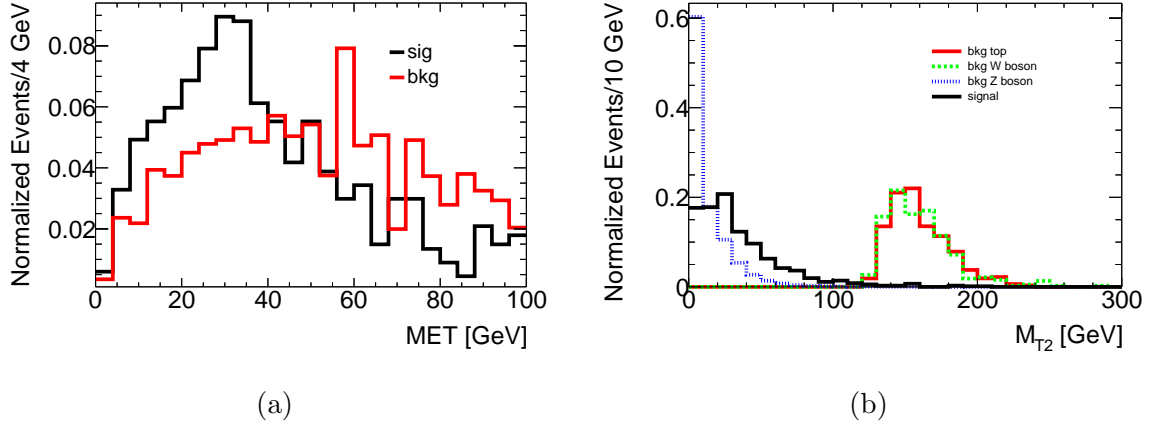


FIG. 7. Normalised distributions in missing transverse energy (a) and M_{T2} (b) for BP4 and backgrounds at the LHC with $\sqrt{s} = 14$ TeV and $L = 300 \text{ fb}^{-1}$. In the right frame we show the three classes of background identified in the text separately.

C. Multivariate analysis

To optimise the signal and background distinction, we exploit a ML analysis, that is, a Gradient-Boosted Decision Tree (GBDT) approach is further applied, which is implemented in the Toolkit for Multivariate Data Analysis (TMVA) with ROOT [48].

A total of ten input variables are used in such a GBDT/TMVA analysis, as listed in Tab. V. In addition to the invariant masses mentioned above, M_{T2} , and H_T , we also compute five angular variables between pairs of final-state objects: $\cos(\theta_{l_1 j_1})$, $\cos(\theta_{l_1 j_2})$, $\cos(\theta_{l_2 j_1})$, $\cos(\theta_{l_2 j_2})$. These angles are defined as the cosine of the angle between the two final states leptons l and jets j , ordered in E_T , and $\cos(\theta_{l_j - l_j})$ is the angle between two reconstructed bound states $(l_j)^1$ and $(l_j)^2$. The distributions are shown in Fig. 8. As seen here, these variables are expected to be particularly useful since, in the signal process, they tend to be collinear due to the underlying boost structure, unlike in the background case.

Energy variables	M_{lj}^1	M_{lj}^2	M_{ll}	M_{jj}	H_T	M_{T2}
Angular variables	$\cos(\theta_{l_j - l_j})$	$\cos(\theta_{l_1 j_1})$	$\cos(\theta_{l_1 j_2})$	$\cos(\theta_{l_2 j_1})$	$\cos(\theta_{l_2 j_2})$	

TABLE V. The input observables used in the GBDT analysis.

In the training stage, we take the signal and ZZ background events as input. Because their physical process are very similar and difficult to distinguish apart in the selection with

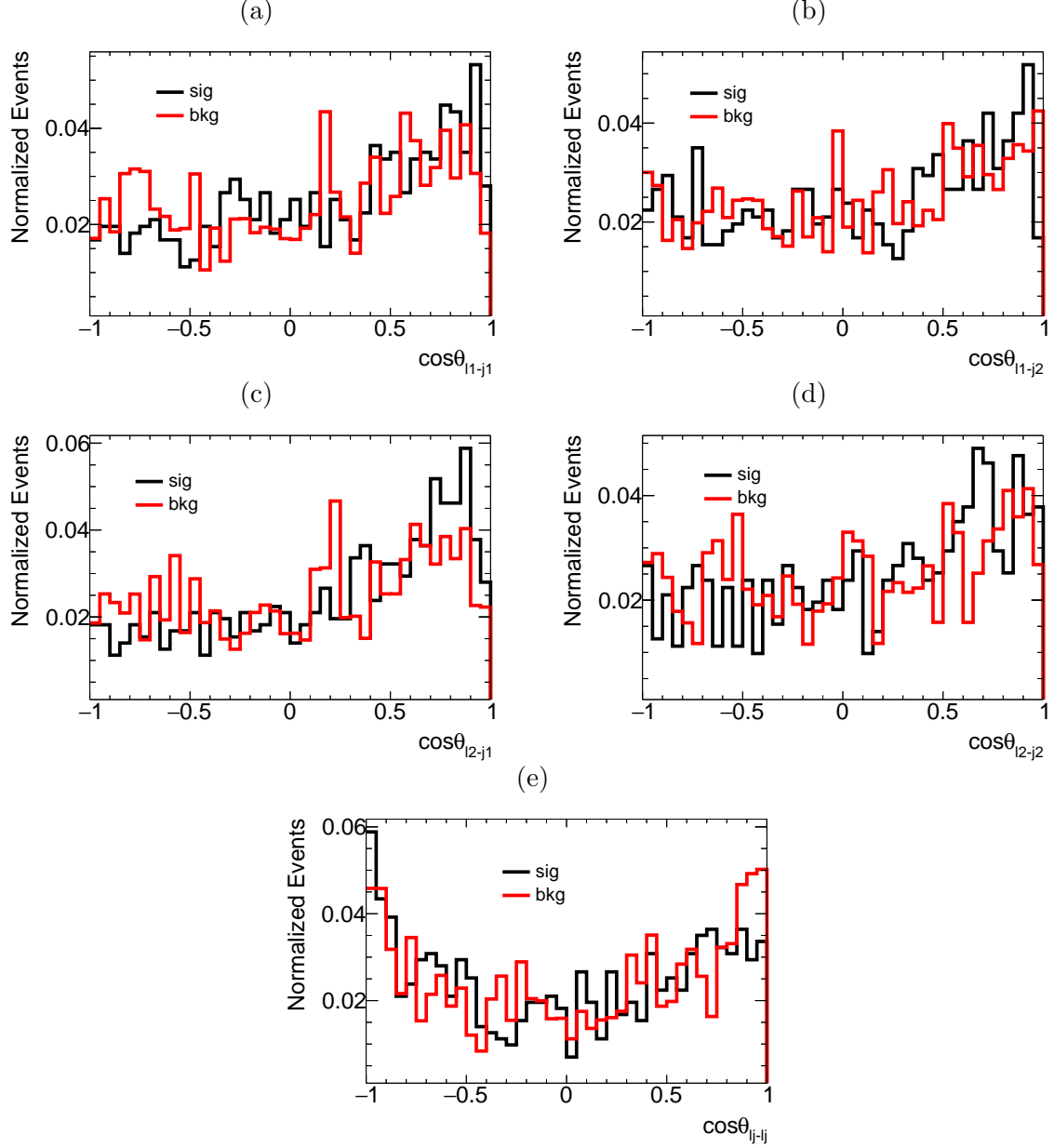


FIG. 8. Normalised distributions in the (cosine of the) angle between pairs of jets/leptons (a)-(d), and two reconstructed bound state $(lj)^1$ and $(lj)^2$ (e) for BP4 and backgrounds at the LHC with $\sqrt{s} = 14$ TeV and $L = 300 \text{ fb}^{-1}$.

kinematic cuts. The M_{T2} and the invariant mass $M_{lj}^{1,2}$ are the most important variables while training. But the angular variables $\cos(\theta_{lj-lj})$ and $\cos(\theta_{l_i j_k})$, $i \neq k$ are also useful. Ultimately, for the GBDT output, a very good separation between the signal and background can be achieved, which is shown in Fig. 9.

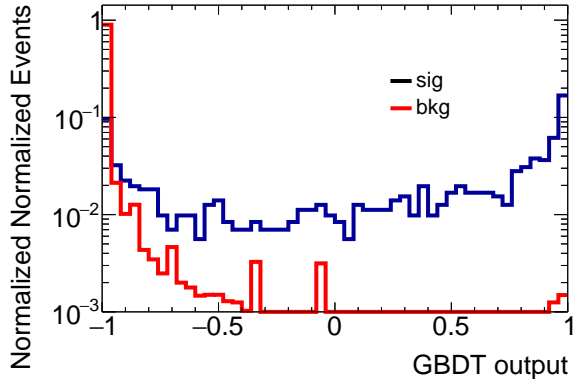


FIG. 9. GBDT output for BP4 and backgrounds.

D. Significances

The process of searching for signals at high-energy colliders using ML techniques is ultimately a statistical process. Therefore, to look for a signal, a large number of events need to be collected, and the kinematic variables of the final-state particles need to be analysed to find differences from the noise, but then a sizeable statistical sample needs to be collected, so as to have enough significance, in order to claim sensitivity to the signal which is being searched for.

The latter is defined here as $\Sigma = \frac{N_S}{\sqrt{(N_S+N_B)}}$, where N_S and N_B represent the number of events for the signal (S) and (total) background (B), respectively, at a given luminosity L .

To distinguish the signal from the backgrounds and to compute the ensuing significance, we apply six kinematic cuts on reconstructed observables and one cut on the GBDT output, the details of which are listed in Tab. VI (for BP4 in the signal case) and where $L = 300 \text{ fb}^{-1}$ (with a centre-of-mass energy of 14 TeV, as usual). Following the acceptance cuts and upon applying the SS lepton criterion (the combination of which we refer to as preselection, hereafter), we see a strong decrease of the initially huge SM backgrounds to the same order as the signal. For example, the troublesome Zjj is almost eliminated after this cut (thus, it is no longer included in this table). As Figs. 4–6 show, the kinematic selection is already quite efficient in separating the signal from the background, especially for the variable M_{T2} . Finally, we also applied a GBDT discrimination before computing the final significances.

$L = 300 \text{ fb}^{-1}$	S	Top quark	W^\pm boson	Z boson	Total background	S/B	Σ
Acceptance	938.2	1.10×10^6	60544.8	2584.9	1.16×10^6	0.008	0.87
SS Leptons	514.8	2970.5	301.4	698.6	3970.4	0.130	7.69
$HT \in [60, 400] \text{ GeV}$	492.8	2743.7	260.6	682.3	3686.5	0.134	7.62
$M_{ll} \in [10, 300] \text{ GeV}$	490.7	2548.3	235	675.7	3459	0.142	7.81
$M_{lj}^1 \in [0, 120] \text{ GeV}$	434.8	1656.5	139.9	486.5	2282.9	0.190	8.34
$M_{lj}^2 \in [0, 150] \text{ GeV}$	415.6	1490.1	123.1	457.6	2070.8	0.20	8.34
$M_{vis} \in [80, 500] \text{ GeV}$	364.7	950.5	88.7	393.1	1432.3	0.255	8.6
$MT^2 \in [10, 110] \text{ GeV}$	293.8	0	0	149.5	149.5	1.965	13.96
GBDT $\in [-0.35, 1]$	247.8	0	0	39.6	56.8	4.363	14.2

TABLE VI. Response to our selection cuts for the signal (BP4) and background (separately and total) rates computed at the LHC with $\sqrt{s} = 14 \text{ TeV}$ and $L = 300 \text{ fb}^{-1}$.

The results on Σ for all 9 BPs are shown in Tab. VII. With only the acceptance and SS lepton criteria, the significances can reach 3. After applying the kinematic cuts, including exploiting the M_{T2} observable, the significances can be even larger than 10. Upon finally applying the GBDT selection, Σ values can increase even further (albeit only slightly). In short, it is clear that a judicious combination of preselection and kinematic cuts combined with a GBDT analysis can result in large sensitivity to a significant expanse of 2HDM Type-X parameter space through our chosen signal at the current LHC stage, already.

Σ	BP1	BP2	BP3	BP4	BP5	BP6	BP7	BP8	BP9
After selecting SS leptons	6.22	5.11	7.71	7.69	5.94	6.42	5.88	8.08	5.4
After kinematic cuts, w/o M_{T2} & GBDT	8.31	7.46	10.71	10.14	8.15	7.91	7.93	10.87	7.78
With M_{T2} , w/o GBDT	11.76	10.81	14.38	13.96	11.54	11.33	11.37	14.65	11.24
With M_{T2} & GBDT	11.91	10.85	14.23	14.20	11.94	11.57	11.52	14.31	11.12

TABLE VII. Significances following our different selections for all signals (BP1-9) at the LHC with $\sqrt{s} = 14 \text{ TeV}$ and $L = 300 \text{ fb}^{-1}$.

V. CONCLUSIONS

In this paper, we have investigated the feasibility of hadro-producing the light Higgs scalar h and pseudoscalar A through Z^* exchange (initiated by $q\bar{q}$ pairs) at the LHC in the 2HDM Type-X (or lepton specific). We have focused on the 4τ final state, where two τ 's decay leptonically to form a pair of SS leptons (electrons and/or muons) and two τ 's decay hadronically (thus producing two jets). We have proven that this kind of signal could be found (or excluded) at the end of Run 3 of the LHC, following a dedicated selection based on both a kinematic and GBDT/TMVA analysis. In order to motivate future studies of this signature, we have also proposed 9 BPs and processed them through a realistic MC analysis for a centre-of-mass energy of 14 TeV and (integrated) luminosity $L = 300 \text{ fb}^{-1}$, thus emulating actual LHC conditions.

ACKNOWLEDGMENTS

SM is supported in part through the NExT Institute and the STFC Consolidated Grant ST/X000583/1. SS is supported in full through the NExT Institute and acknowledges the use of the IRIDIS High Performance Computing Facility, and associated support services, at the University of Southampton, in the completion of this work. YW's work is supported by the Natural Science Foundation of China Grant No. 12275143, and the Fundamental Research Funds for the Inner Mongolia Normal University Grant No. 2022JBQN080. QSY is supported by the Natural Science Foundation of China under the Grants No. 11875260 and No. 12275143.

-
- [1] G. Aad *et al.* [ATLAS], Phys. Lett. B **716** (2012) 1, [arXiv:1207.7214 [hep-ex]].
 - [2] S. Chatrchyan *et al.* [CMS], Phys. Lett. B **716** (2012) 30, [arXiv:1207.7235 [hep-ex]].
 - [3] G. Aad *et al.* [ATLAS], Nature **607**, no.7917, 52-59 (2022) [erratum: Nature **612**, no.7941, E24 (2022)] [arXiv:2207.00092 [hep-ex]].
 - [4] A. Tumasyan *et al.* [CMS], Nature **607**, no.7917, 60-68 (2022) [arXiv:2207.00043 [hep-ex]].
 - [5] T. D. Lee, Phys. Rev. D **8** (1973), 1226-1239.
 - [6] N. G. Deshpande and E. Ma, Phys. Rev. D **18** (1978), 2574.

- [7] G. C. Branco, P. M. Ferreira, L. Lavoura, M. N. Rebelo, M. Sher and J. P. Silva, Phys. Rept. **516** (2012), 1-102 [arXiv:1106.0034 [hep-ph]].
- [8] S. L. Glashow and S. Weinberg, Phys. Rev. D **15** (1977), 1958
- [9] M. Aoki, S. Kanemura, K. Tsumura and K. Yagyu, Phys. Rev. D **80**, 015017 (2009) [arXiv:0902.4665 [hep-ph]].
- [10] V. Khachatryan *et al.* [CMS], JHEP **01**, 079 (2016) [arXiv:1510.06534 [hep-ex]].
- [11] V. Khachatryan *et al.* [CMS], JHEP **10**, 076 (2017) [arXiv:1701.02032 [hep-ex]].
- [12] A. M. Sirunyan *et al.* [CMS], Phys. Lett. B **800**, 135087 (2020) [arXiv:1907.07235 [hep-ex]].
- [13] T. Albahri *et al.*, Phys. Rev. D **103** (2021), 072002
- [14] A. Jueid, J. Kim, S. Lee, and J. Song, Phys. Rev. D **104** (2021), no. 9 095008 [arXiv:2104.10175].
- [15] A. M. Sirunyan *et al.* [CMS], CMS-PAS-SUS-23-007".
- [16] A. Arhrib, R. Benbrik, M. Krab, B. Manaut, S. Moretti, Y. Wang and Q. S. Yan, JHEP **10**, 073 (2021) [arXiv:2106.13656 [hep-ph]].
- [17] Y. Wang, A. Arhrib, R. Benbrik, M. Krab, B. Manaut, S. Moretti and Q. S. Yan, JHEP **12**, 021 (2021) [arXiv:2107.01451 [hep-ph]].
- [18] A. Arhrib, R. Benbrik, M. Krab, B. Manaut, S. Moretti, Y. Wang and Q. S. Yan, Symmetry **13**, no.12, 2319 (2021) [arXiv:2110.04823 [hep-ph]].
- [19] Z. Li, A. Arhrib, R. Benbrik, M. Krab, B. Manaut, S. Moretti, Y. Wang and Q. S. Yan, [arXiv:2305.05788 [hep-ph]].
- [20] D. Eriksson, J. Rathsman and O. Stål, Comput. Phys. Commun. **181** (2010), 189-205 [arXiv:0902.0851 [hep-ph]].
- [21] S. Kanemura, T. Kubota and E. Takasugi, Phys. Lett. B **313**, 155-160 (1993) [arXiv:hep-ph/9303263 [hep-ph]].
- [22] A. G. Akeroyd, A. Arhrib and E. M. Naimi, Phys. Lett. B **490**, 119-124 (2000) [arXiv:hep-ph/0006035 [hep-ph]].
- [23] A. Arhrib, [arXiv:hep-ph/0012353 [hep-ph]].
- [24] S. Kanemura, T. Kubota and E. Takasugi, Phys. Lett. B **313** (1993), 155-160 [arXiv:hep-ph/9303263 [hep-ph]].
- [25] A. G. Akeroyd, A. Arhrib and E. M. Naimi, Phys. Lett. B **490** (2000), 119-124 [arXiv:hep-ph/0006035 [hep-ph]]. A. Arhrib, [arXiv:hep-ph/0012353 [hep-ph]].

- [26] M. E. Peskin and T. Takeuchi, Phys. Rev. Lett. **65** (1990), 964-967.
- [27] M. E. Peskin and T. Takeuchi, Phys. Rev. D **46** (1992), 381-409.
- [28] R. L. Workman *et al.* [Particle Data Group], PTEP **2022**, 083C01 (2022)
- [29] P. Bechtle, D. Dercks, S. Heinemeyer, T. Klingl, T. Stefaniak, G. Weiglein and J. Wittbrodt, Eur. Phys. J. C **80** (2020) no.12, 1211 [arXiv:2006.06007 [hep-ph]].
- [30] P. Bechtle, S. Heinemeyer, T. Klingl, T. Stefaniak, G. Weiglein and J. Wittbrodt, Eur. Phys. J. C **81** (2021) no.2, 145 [arXiv:2012.09197 [hep-ph]].
- [31] F. Mahmoudi, Comput. Phys. Commun. **180** (2009), 1579-1613 [arXiv:0808.3144 [hep-ph]].
- [32] E. J. Chun and J. Kim, JHEP **07** (2016) 110.
- [33] S. M. Barr and A. Zee, Phys. Rev. Lett. **65**, 21 (1990).
- [34] V. Ilisie, JHEP **04** (2015) 077.
- [35] Y. S. Amhis *et al.* [HFLAV], Phys. Rev. D **107**, no.5, 052008 (2023) [arXiv:2206.07501 [hep-ex]].
- [36] R. Aaij *et al.* [LHCb], Phys. Rev. D **105**, no.1, 012010 (2022) [arXiv:2108.09283 [hep-ex]].
- [37] R. Aaij *et al.* [LHCb], Phys. Rev. Lett. **128**, no.4, 041801 (2022) [arXiv:2108.09284 [hep-ex]].
- [38] A. Tumasyan *et al.* [CMS], Phys. Lett. B **842**, 137955 (2023) [arXiv:2212.10311 [hep-ex]].
- [39] J. Alwall, R. Frederix, S. Frixione, V. Hirschi, F. Maltoni, O. Mattelaer, H. S. Shao, T. Stelzer, P. Torrielli and M. Zaro, JHEP **07** (2014), 079 [arXiv:1405.0301 [hep-ph]].
- [40] T. Sjostrand, S. Mrenna and P. Z. Skands, JHEP **05** (2006), 026 [arXiv:hep-ph/0603175 [hep-ph]].
- [41] T. Sjöstrand, S. Ask, J. R. Christiansen, R. Corke, N. Desai, P. Ilten, S. Mrenna, S. Prestel, C. O. Rasmussen and P. Z. Skands, Comput. Phys. Commun. **191** (2015), 159-177 [arXiv:1410.3012 [hep-ph]].
- [42] J. de Favereau *et al.* [DELPHES 3], JHEP **02** (2014), 057 [arXiv:1307.6346 [hep-ex]].
- [43] M. Cacciari, G. P. Salam and G. Soyez, JHEP **04**, 063 (2008) [arXiv:0802.1189 [hep-ph]].
- [44] M. Cacciari, G. P. Salam and G. Soyez, Eur. Phys. J. C **72**, 1896 (2012) [arXiv:1111.6097 [hep-ph]].
- [45] A. Arhrib, S. Moretti, S. Semlali, C. H. Shepherd-Themistocleous, Y. Wang and Q. S. Yan, Phys. Rev. D **109**, no.5, 055020 (2024) [arXiv:2310.02736 [hep-ph]].
- [46] C. G. Lester, D. J. Summers, Physics Letters B **463.1** (1999): 99-103. [arXiv:9906349 [hep-ph]].

- [47] A. Barr, C. Lester and P. Stephe, *Journal of Physics G: Nuclear and Particle Physics*, 29(10), 2343 [arXiv:0304226 [hep-ph]].
- [48] J. Therhaag, *PoS ICHEP2010* (2010), 510